Optical Materials 157 (2024) 116135

Contents lists available at ScienceDirect

Optical Materials

journal homepage: www.elsevier.com/locate/optmat

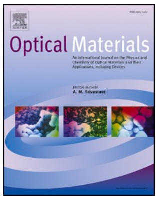

Synergetic experimental and theoretical investigation of molecular structure – Optical properties relationships of anthrazoline-based polymeric chains

Irina A. Shchugoreva [a,b], Ruslan Y. Smyslov [c,d,*], Irina A. Nasirova [c], Mikhail Y. Goikhman [c], Alexander V. Yakimansky [c], Sergei G. Ovchinikov [e], Polina V. Artyushenko [a,b], Anastasia V. Rogova [a,b], Felix N. Tomilin [a,e,**], Pavel V. Avramov [f,***]

[a] *Laboratory for Digital Controlled Drugs and Theranostics, Krasnoyarsk Scientific Center, Siberian Branch, Russian Academy of Sciences, Akademgorodok 50, Krasnoyarsk, 660036, Russia*

[b] *Krasnoyarsk State Medical University, ul. Partizana Zheleznyaka 1, Krasnoyarsk, 660022, Russia*

[c] *Branch of Petersburg Nuclear Physics Institute named by B.P.Konstantinov of National Research Centre «Kurchatov Institute» – Institute of Macromolecular Compounds, Bolshoy pr-t 31, St. Petersburg, 199004, Russia*

[d] *Institute of Biomedical Systems and Biotechnology, Graduate School of Biomedical Systems and Technology, Peter the Great St. Petersburg Polytechnic University, St. Petersburg, 195251, Russia*

[e] *Kirensky Institute of Physics, Krasnoyarsk Scientific Center, Russian Academy of Sciences, Siberian Branch, Akademgorodok 50, Krasnoyarsk, 660036, Russia*

[f] *Department of Chemistry and Green-Nano Materials, Research Center, Kyungpook National University, 80 Daehakro, Bukgu, Daegu, 41556, Republic of Korea*

ARTICLE INFO

Keywords:
Polyamides
Electronic structure
Induction effect
Mesomeric effect
Time-depending density functional theory TD-DFT
B3LYP

ABSTRACT

The photoluminescence and UV–Vis absorption spectra of copolyamides containing 1,9-anthrazoline with para- and meta-[(substituted carbonyl)amino]phenyl-1-ene moieties in a polymer backbone were studied by a combination of experimental and theoretical approaches. The investigation was accomplished through time-dependent density functional theory electronic structure calculations of small-molecule models mimicking a polymer chain. Theoretical absorption and luminescence spectra of ten atomistic models were compared with corresponding experimental data, and the optical properties of two new luminescent molecules with bromine auxochrome were predicted. An analysis of the optical properties demonstrate an identical effect of the type and position of a substituent on the spectra for para- and meta-[(substituted carbonyl)amino]phenyl-1-ene moieties. It was found that the absorption and luminescence spectra of theoretical para-models demonstrate red shifts relative to the corresponding meta-ones. The same phenomenon was observed in experimental spectra of low-molecular-mass compounds and corresponding copolyamides in solution and bulk. Unique optical properties allow anthrazoline-based polymer compounds to be used in numerous advanced optoelectronic applications with desired optical and electronic characteristics.

1. Introduction

The field of molecular electronics has significantly impacted modern technology, and organic semiconductors, a result of extensive research in this area, have proved to be highly valuable [1]. These semiconductors possess favorable characteristics such as flexibility [2], low cost [3], and intrinsic properties like light emission [4], making them suitable for a wide range of applications. Organic semiconductors have been demonstrated to have significant utility in a number of technological applications, including organic light-emitting diodes (OLEDs), photovoltaic cells, thin film transistors, and biosensors. The majority of materials employed in these applications often comprise conjugated

---

* Corresponding author. Branch of Petersburg Nuclear Physics Institute named by B.P.Konstantinov of National Research Centre «Kurchatov Institute» – Institute of Macromolecular Compounds, Bolshoy pr-t 31, St. Petersburg, 199004, Russia.

** Corresponding author. Kirensky Institute of Physics, Krasnoyarsk Scientific Center, Russian Academy of Sciences, Siberian Branch, Akademgorodok 50, Krasnoyarsk, 660036, Russia.

*** Corresponding author.

E-mail addresses: urs@macro.ru (R.Y. Smyslov), felix@iph.krasn.ru (F.N. Tomilin), paul.veniaminovich@knu.ac.kr (P.V. Avramov).

https://doi.org/10.1016/j.optmat.2024.116135
Received 20 June 2024; Received in revised form 25 August 2024; Accepted 16 September 2024

π-systems, as evidenced by previous research [5–7].

Nitrogen-containing heterocycles, including anthrazolines, are highly intriguing among the numerous conjugated compounds that exhibit luminescence within the visible spectral range [8–10]. They are small, conjugated π-electron molecules, with high electron affinity, high thermal stability, and n-type semiconductors properties [11,12]. In particular, modern synthesis methods enable the formation of anthrazoline compounds with diverse chemical structures, as well as the incorporation of functional groups required for the preparation of high-molecular-weight compounds into these heterocycles [13]. Fine-tuning of the optical characteristics of chromophore-containing polymers can be accomplished by changing the position of the functional groups along a side chain.

The synthesis of anthrazoline and its derivatives can be challenging because of various factors. Key difficulties include the complex molecular structure of anthrazoline compounds, limited availability of starting materials, low reactivity, stereochemistry and regioselectivity issues, and purification challenges [14]. To overcome these challenges, careful design and optimization of reaction conditions, development of efficient synthetic routes, use of specialized reagents or catalysts, and advanced purification techniques may be required. Thus, before the complex chemical synthesis of conjugated oligomers and corresponding polymers [15], it would be useful to predict absorption and photoluminescence (PL) properties in ultraviolet (UV), visible, and infrared (IR) spectral regions using state-of-the-art quantum-chemical approaches [16–19]. Selçuk Gümüş and Murat Akbay conducted a study to investigate the effects of chemical modification on the aromaticity of diazaanthracene through the introduction of F, Cl, OH, and NO_2 substituents. They used electronic structure calculations [20] and found that the reduction in the aromaticity of the parent diazaanthracene can be compensated by the presence of an electronegative atom substituent. In fact, the aromaticity is determined by the position of a substituent: the closer to the nitrogen atoms, the higher the aromaticity of anthracene moiety.

It is known that for macromolecules in solution and in bulk, it is necessary to consider the effects of interactions of distant contacts along the chain, intermacromolecular interactions to account for energy transfer phenomena, the possibility of forming charge transfer complexes, as well as excimers and exciplexes [21]. As a result, a state-of-the-art quantum-chemical interpretation of optoelectronic properties of polymers in solutions, monoliths, and melts is a challenging task. The present study introduces a novel approach for examining the optoelectronic properties of copolyamides incorporating anthrazoline. This is achieved through the utilization of quantum chemical computations, wherein a simplified molecular model is employed to represent the polymer chain. To investigate the optoelectronic properties of anthrazoline derivatives, the study considered both low-molecular-mass compounds in solution, as well as polymeric chains in solutions and films. This investigation was conducted through a combination of experimental and theoretical approaches. The main objective of the study is to interpret of UV–Vis absorption and photoluminescence (PL) spectra of high-molecular-mass anthrazoline-containing copolyamides (coPA) and their low-molecular-mass synthetic compounds (LMM, Fig. S1) imitating structural repeating units (SRU) based on quantum-chemical simulations of theoretical structural models (Table 1). The effects of substituents, including methyl and carboxylic groups, Br, and their combinations, on the energy gaps and energy levels of the frontier orbitals of luminophore moieties of coPAs were determined. These effects were studied and interpreted using the theoretical approach [22].

2. Materials and methods

2.1. Purification of initial compounds and solvents

Chloral hydrate; hydroxylamine hydrochloride; *m*-phenylenediamine hydrochloride; *p*-aminoacetophenone; *m*-aminoacetophenone; 4,4-oxydianiline (IUPAC name 4-(4-aminophenoxy) aniline); terephthalic acid (IUPAC name benzene-1,4-dicarboxylic acid); vanillic acid

Table 1
Designations of copolyamides and model compounds and atomic structure for theoretical models containing 1,9-anthrazoline cores with para(*p*)-|meta(*m*)-[(substituted carbonyl)amino]phenyl-1-ene and different combinations of auxochromes.

Theoretical model structure[1] with			
p-phenylenes		*m*-phenylenes	
Symbol	Formula	Symbol	Formula
M1p	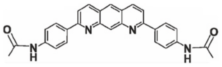	M1m	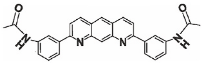
M2p	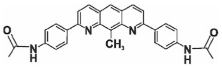	M2m	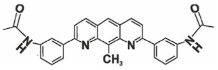
M3p	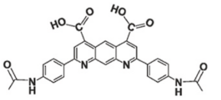	M3m	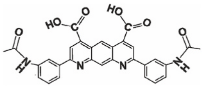
M4p	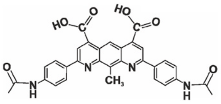	M4m	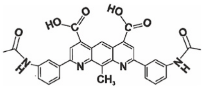
M5p	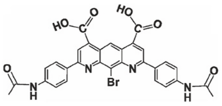	M5m	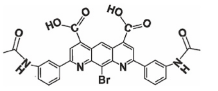
M6p	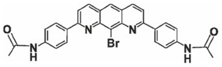	M6m	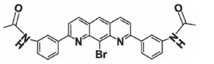

---

[1] The Marvin code [31] was used for drawing and displaying chemical structures and substructures.

Table 2

Theoretical and experimental spectral positions of the absorption (λ_{abs}) and photoluminescence peaks (λ_{lum}) for theoretical models, low-molecular-mass synthetic compounds, and polyamides as a function of the different substituted 1,9-anthrazoline cores with para(*p*)- and meta(*m*)-[(substituted carbonyl)amino]phenyl-1-ene and different combinations of auxochromes.

Combination[a]	UV–Vis absorption (λ_{abs}, nm)[b]			Photoluminescence (λ_{lum}, nm)[c]			
	Theoretical Model[d]	LMM[d] Compounds (in NMP)	Polymer[d] (in NMP)	Theoretical Model	LMM Compounds (in NMP)	Polymer (in NMP)	Polymer (film)
p-cogiguration for M{1–6}p, L{1–6}p, and P{1–6}p[d]							
1p[e]	410	443	399 (sh),[f] 414, 457 (ed)[g]	441	578	495, 576	638
2p	407	436	391, 412 (sh), 428 (ed)	437	573	476, 550 (sh)	480 (sh), 581, 630 (sh)
3p	463	473	411, 447 (ed)	515	662	501, 540 (sh)	503, 586 (sh), 650 (sh)
4p	454	471	396 (sh), 424 (sh), 443 (ed)	519	658	500, 550 (sh)	503 (sh), 532, 580 (sh)
5p	470	458	428, 470 (ed)	523	588	517, 545	507 (sh), 590 (sh), 619
6p	412	–	–	452	–	–	–
m-cofiguration for M{1–6}m, L{1–6}m, and P{1–6}m							
1m[e]	384	391, 401 (sh)	378, 395, 412 (ed)	423	498	427 (sh), 447	428 (sh), 456, 483 (sh) 567 (sh), 617 (sh)
2m	379	399	379(sh), 397 (sh), 425 (ed)	509	514	443 (sh), 467	441 (sh), 472 (sh), 497, 525 (sh)
3m	428	400, 430 (sh)	392, 408, 433 (ed)	489	520	494	493, 533 (sh), 562
4m	427	407, 437 (sh)	387 (sh), 408 (sh), 437 (ed)	508	504	503	511, 550 (sh), 617 (sh)
5m	443	408, 450 (sh)	383 (sh), 402 (sh), 430 (ed)	499	495	503	508 (sh), 546 (sh), 579 (sh), 612, 657 (sh)
6m	391	–	–	446	–	–	–

[a] Auxochromic combinations in an anthrazolene core.

[b] λ_{abs} is the wavelength of the $S_0 \rightarrow S_1$ transition in the absorption band maximum.

[c] λ_{lum} is the wavelength of the $S_0 \leftarrow S_1$ transition in the emission band maximum.

[d] Designations for the studied objects: theoretical models (M), low-molecular-mass synthetic compounds (L), and polymers (P) of quantum-chemical calculations.

[e] p and m designate para and meta positions, respectively.

[f] Abbreviation 'sh' means a shoulder in the experimental spectra.

[g] ed means an absorbance band edge at $A = 0.3$. The spectral maxima and shoulders shown in the table are derived from deconvolution of the absorption and luminescence spectra (see Fig. S3, Tables S4 and S5).

(products of Sigma-Aldrich); anhydrous sodium sulfate; sulfuric acid 98 %; bromine 99 %; caustic potash; hydrochloric acid 37 %; thionyl chloride 97 %; Sodium bisulfite (Vekton Products) was used without additional purification.

Solvents: ethanol 96 %; diethyl ether 99 %; dimethyl sulfoxide (DMSO) 99 % (Vekton Products) was used without additional purification; N-methylpyrrolidone (NMP), $T_{bp} = 202°C$, $n_D^{20} = 1.4692$, dried over calcium hydride and distilled under vacuum (5 mm Hg, $T_{bp} = 65°C$); N,N-dimethylformamide (DMF), $T_{bp} = 153°C$, $n_D^{20} = 1.4269$, dried over calcium hydride and distilled under vacuum (5 mm Hg, $T_{bp} = 38°C$); pyridine, $T_{bp} = 115°C$, $n_D^{20} = 1.5095$, dried over granular potassium hydroxide and purified by simple distillation.

2.2. Synthesis of intermediates

2H,3H,5H,6H-benzo [1,2-b:5,4-b']dipyrrole-2,3,5,6-tetraone 1 was synthesized in two stages by the Sandmeyer reaction following procedure described in Ref. [23].

2.3. Synthesis of 8-bromopyrrolo[3,2-f]indole-2,3,5,6(1H,7H)-tetraone 2

7 mL of concentrated sulfuric acid was placed in a three-necked round bottom flask with a stopper, reflux condenser, and an addition funnel, and was cooled to −8 °C. Thereafter, 1.6 g (7.5 mmol) of 8-methylpyrrolo[3,2-f]indole-2,3,5,6(1H, 7H)-tetraone (bis-isatin) was slowly added until it was completely dissolved. Consequently 0.4 mL (7.7 mmol) of bromine was added dropwise upon keeping the temperature below 0 °C. The mixture was slowly (during 2 h) heated to 30°C and 0.4 mL (7.7 mmol) of bromine was added. After that the solution was kept at 60°C temperature for 24 h. Excess bromine was removed with an air flow and the reaction mixture was poured into ice water containing a small amount of sodium bisulfite to absorb the remaining bromine. The obtained dark-orange precipitate was filtered off, washed with water, and dried at 60 °C. The yield of 8-bromopyrrolo[3,2-f]indole-2,3,5,6(1H, 7H)-tetraone 2 was 1.0 g (45 %), ^{1}H NMR (DMSO-d_6), δ (ppm): 7.62 (1H, c, C_{ArH}); 11.90 (2H, c, NH).

2.4. Monomer and polymer synthesis

The synthesis of terephthaloyl bis(3-methoxy-4-hydroxybenzoic) acid dichloride was performed according to the procedure described in Ref. [24].

The synthesis of 2,8-bis(4-aminophenyl)pyrido [3,2-g]quinoline-4,6-dicarboxylic acid, 2,8-bis(3-aminophenyl)pyrido [3,2-g]quinoline-4,6-dicarboxylic acid, 2,8-bis(4-aminophenyl)-10-bromopyrido [3,2-g]quinoline-4,6-dicarboxylic acid, 2,8-bis(3-aminophenyl)-10-bromopyrido [3,2-g]quinoline-4,6-dicarboxylic acid, 2,8-bis(4-aminophenyl)-10-methylpyrido [3,2-g]quinoline-4,6-dicarboxylic acid, 2,8-bis(3-aminophenyl)-10-methylpyrido [3,2-g]quinoline-4,6-dicarboxylic acid was carried out by the Pfitzinger reaction according to the procedure from Ref. [23].

The synthesis of 4,4'-(pyrido [3,2-g]quinoline-2,8-diyl)dianiline, 3,3'-(pyrido [3,2-g]quinoline-2,8-diyl)dianiline, 4,4'-(10-methylpyrido [3,2-g]quinoline-2,8-diyl)dianiline and 3,3'-(10-methylpyrido [3,2-g]quinoline-2,8-diyl)dianiline was carried out by the decarboxylation reaction of the corresponding dicarboxylic acids [23].

The copolymers were synthesized by the conventional method [13].

2.5. Photoluminescence and absorption UV–Visible spectra of antrozoline and its polymeric chains

The coPA solutions with anthrazoline units in the main chain in N-methylpyrrolidone, as well as the low-molecular-mass synthetic models of fluorescent groups were studied using both absorption UV–Vis and photoluminescence spectroscopy. The concentrations of LMM and SRU in coPAs were 0.007 and 0.06 mg/mL in NMP respectively. Then, the molar concentrations of LMM and coPA anthrazoline groups consisted of 30 μM and 15 μM respectively. The coPA films created by pouring NMP solutions with concentration 10 mg/mL were used to record PL and UV–Vis spectra.

The photoluminescent spectra of coPA and their synthetic models were recorded using an LS-100 BASE luminescence spectrophotometer (PTI® Lasers INC, Canada). The luminescence intensity I_{lum} of the coPA films was detected in the fluorescence mode from the side of incidence of the exciting light beam in the phosphorescence mode using a solid sample holder. The grazing angle of the excitation light beam to the sample was ~30°. The wavelength range of the emission spectra was 400–750 nm at an excitation wavelength of $\lambda_{\mathrm{exc}} = 380$ nm. The spectral widths of excitation and luminescence monochromator slits were 4 nm. To ensure the correct comparison, the I_{lum} values were reduced to an internal laboratory standard. The absorption spectra were obtained on an SF-256 UVI spectrophotometer (LOMO Photonics, Russia) in the wavelength range of 300–650 nm. The absorption and luminescent spectra were treated and deconvoluted using the OriginPro 2024b code [25].

2.6. Calculation details

The electronic structure of all the molecular species was calculated using direct space density functional theory (DFT) approach. The atomic structures of all theoretical models in the ground and excited states were optimized using the B3LYP hybrid functional [26] with cc-pVDZ basis set, considering the methanol by SMD implicit solvation model [27]. This solvent was chosen since its permittivity ($\varepsilon = 32.6$) is comparable to the value for 1-methylpyrrolidin-2-one ($\varepsilon = 32.0$) used in the experiment. Once the geometry optimization is completed, the next step was to verify the atomic structures by Hessian calculation. Based on the obtained structures the absorption and luminescence spectra were calculated on the TD/SMD/B3LYP/cc-pVDZ level of theory [28] (see more details in Fig. S2 and its description). All the calculations were performed using the GAMESS software package [29]. Optimization procedure followed the algorithm [30] for low-dimensional lattices.

In this study, ten quantum chemical models are proposed to compare their optical properties with those of the previously synthesized LMM [13] that are diamines, i.e., bifunctional monomers for the low-temperature polycondensation (Table 1). These theoretical structural models similar to the experimental photoactive bifunctional monomers are with para (p) (M1p−M5p) and meta (m) (M1m−M5m) configurations (Table 1 and Tables S2 and S3)—M stands for theoretical models—to elucidate the effect of substituents' combination and the conjugation effects on their optical properties. The compounds synthesized are divided into two groups with para (L1p−L5p) and meta (L1m−L5m) configurations for phenylene moieties of anthrazoline-containing fragments (here L denotes LMM) having the five auxochromic substituents' combinations synthesized (Fig. S1). Two theoretical structures (M6p|m, Table 1) never synthesized before were introduced for theoretical examination. In Ref. [13], the optical properties of copolymers P1p–P5p and P1m–P5m (P denotes polymers) with similar chromophore groups (Table 1) were synthesized and studied.

3. Results and discussion

3.1. Optical properties of theoretical models

For the sake to study polymer optical properties, the electronic structure calculations of theoretical M1p molecular model (Table 1) in para- and meta-phenylene configuration in the anthrazoline core were performed at B3LYP/cc-pVDZ level of theory in the framework of SMD model for methanol environment. The nature of electron excitations is determined by HOMO-1 and LUMO molecular orbitals since TD/SMD/B3LYP/cc-pVDZ calculations demonstrated the main (90 %) contribution of the orbitals to the $S_0 \rightarrow S_1$ transition intensities (Table S1). It was found that the anthrazoline core is responsible for the M1p photoluminescence since mostly LUMOs are localized at this fragment (Fig. 1). The calculated absorption and luminescence spectra have a maximum at a wavelength of 410 and 441 nm, respectively (Fig. 1, Table 2).

The presence of methyl group in position 10 of the anthrazoline core in M2p molecule leads to a slight shift of the absorption and photoluminescence spectra to the short-wavelength region (hypsochromic effect) relative to the M1p spectra with wavelengths 407 and 437 nm, respectively (Table 2, Fig. 1). The Löwdin atomic charge [20,32] of the methyl group is equal to + 0.05 e^{-} for the overall methyl group, i.e. methyl radical serves as an electron donor with a positive σ-inductive effect, + I_{σ}, (Table S2) increasing the electron density localized at anthrazoline group and degree of binary bonding with consequent reduction of conjugation nature [33].

The presence of two carboxyl groups in M3p leads to a bathochromic shift of theoretical UV–Vis absorption and photoluminescence spectra relative to M1p and M2p ones (Table 2, Fig. 1). The carboxyl substituent is an electron acceptor and exhibits a negative mesomeric effect, –*M*, which is confirmed by the Löwdin atomic charges (Table S2) [33]. The carboxyl group attracts anthrazoline core π-conjugation electrons which leads to electron density delocalization and increasing of anthrazoline-containing fragment's conjugation. The electronic excitations of the electronic states localized at carboxyl groups lead to formation of π-orbitals localized at anthrazoline core (M3p LUMO, Fig. 1). It directly indicates additional delocalization of the electron density at anthrazolinic fragment and increasing of conjugation of M3p excited state, which agrees well with theoretical red shift in the emission spectra.

M4p molecule (Table 1) has both donor ($-CH_3$) and acceptor (–COOH) groups. The effect of the multidirectional substituents on the electron density of the anthrazoline fragment leads to a bathochromic shift of the absorption and luminescence spectra relative to M1p with the maxima wavelengths of absorption and photoluminescence spectra at 454 and 519 nm, respectively (Table 2, Fig. 1). The spectral maxima and shoulders shown in the table are derived from deconvolution of the experimental absorption and photoluminescence spectra (Fig. S3, Tables S4 and S5).

The presence of –Br substituent in the M5p compound as compared to M3p (Table 1) leads to a bathochromic shift of the spectra with absorption and photoluminescence wavelengths of 470 and 523 nm, respectively (Table 2, Fig. 1). This leads to a small delocalization of electronic density at the anthrazoline core in comparison with M3p accompanied with an increase in conjugation of π-electronic system caused by compensation of –*I* and +*M* effects for bromine substituent. The latter occurs because of conjugation of one of the bromine's lone electron pairs with a π-electron system of anthrazoline core and this conjugation is more effective, the closer in energy are the orbitals of carbon and a heteroatom. The combined effects of +*M* and –*I* could also give a negative net charge with Br charge to be ca. 0.1 e^{-} making it an electron donor (Table S2).

The minor bathochromic effect in UV–Vis (from 410 to 412 nm) is also found in the transition from the M1p to the M6p with bromine atom in position 10 of the anthrazoline core. The photoluminescence spectra also demonstrate minor bathochromic effect from 441 to 452 nm

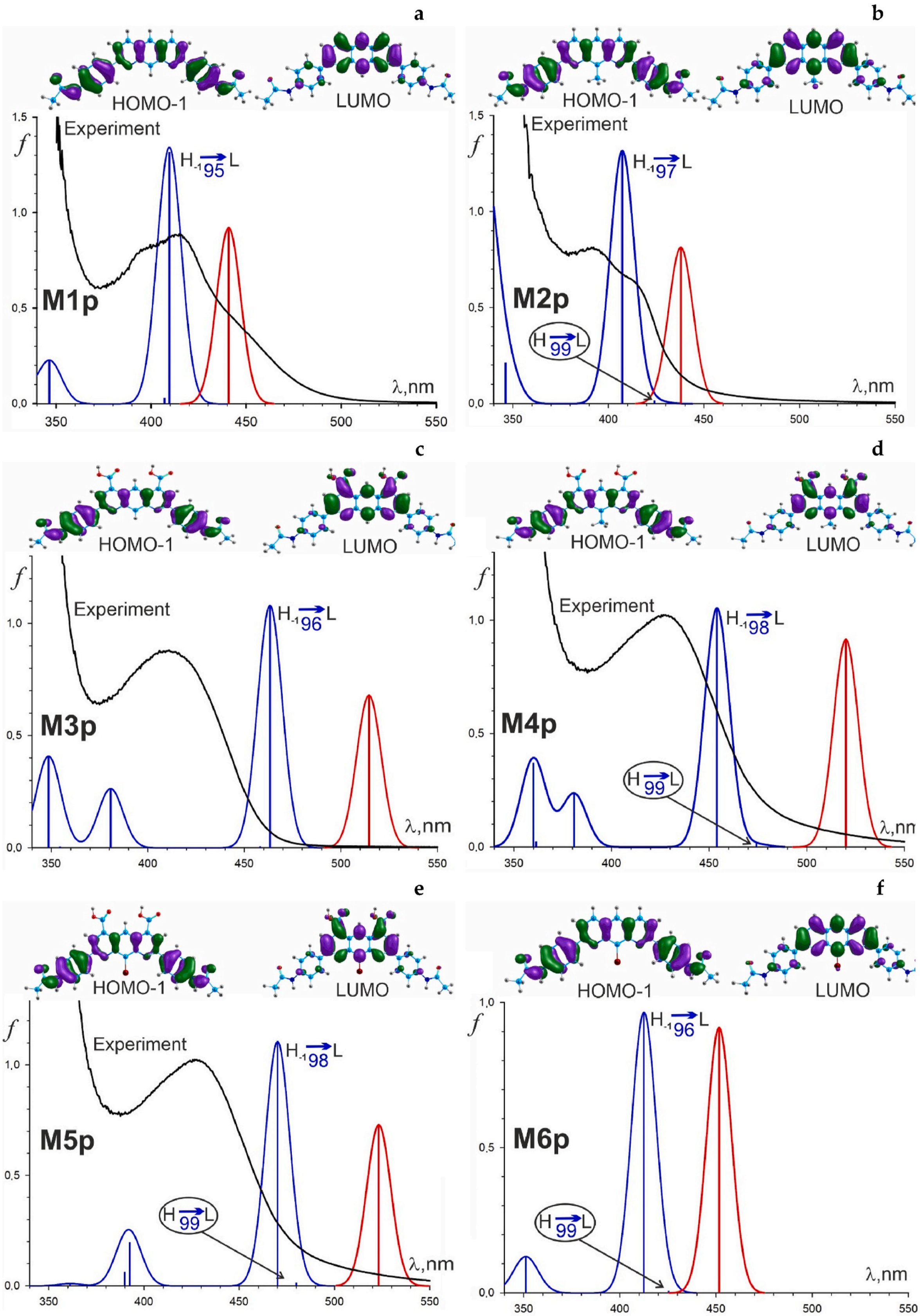

Fig. 1. The theoretical absorption (blue) and emission (red) spectra of M1p–M6p molecules and experimental absorption spectra (black) of P1p–P5p polymers in NMP solution (a–f, respectively). H_{-1} stands for HOMO-1, H is for HOMO, and L is for LUMO orbitals with contribution (%) in different transitions. Oscillator strength, *f*, is in arb. un. Theoretical spectral profiles were simulated using Gaussian functions with a full width at half maximum (FWHM) of 15 nm.

(Table 2, Fig. 1). As in the M5p compound, the Br atom exhibits the donor properties with Löwdin atomic charge equal to 0.10 e^- (Table S2).

The maxima wavelengths of absorption and luminescence spectra of M1m (Fig. 2) in meta configuration are equal to 384 and 423 nm, respectively, which agree well with the experimental data for P1m in NMP (Table 2) with HOMO-1 and LUMO states responsible for $S_0 \rightarrow S_1$ transitions. However, unlike the compounds in the para configuration, for all MNm systems, the HOMO-1 electron density is localized mainly on phenylene rings like in M1m, whereas the LUMO state is localized mainly on the anthrazoline group (Fig. 2).

The maximum of photoluminescence spectrum of M2m with a methyl substituent group being in position 10 of the anthrazoline core (Table 2, Fig. 2) demonstrates minor hypsochromic effect relative to M1m spectrum with absorption and photoluminescence wavelengths equal to 379 and 509 nm, respectively. The methyl group Löwdin charge is 0.04 e^- (Table S3), with increased negative charge localized at anthrazoline fragment up to -0.16 e^- in comparison with M1m without the substituents ($-$ 0.03 e^-).

The introduction of two carboxyl groups into M3m anthrazoline core leads to red shifts of the maxima in the absorption (428 nm) and photoluminescence (489 nm) spectral bands in respect to M1m (384 and 423 nm, respectively). According to the Löwdin atomic charges (Table S3), carboxyl groups exhibit the acceptor properties and the total charge on anthrazoline became positive (0.02 e^-). M4m spectra exhibits a bathochromic shift relative to M1m with absorption and luminescence wavelengths of 427 and 507 nm, respectively, due to the presence of both donor –CH_3 and acceptor –COOH substituents in the structure.

The introduction of the bromine substituent in both M1m and M3m, with the latter containing two carboxyl groups in the anthrazoline core, leads to the bathochromic effect observed for M6m and M5m as well in absorption and photoluminescence spectra (Table 2, Fig. 2). According to Löwdin atomic charges, bromine exhibits the donor properties (Table S3).

A hypsochromic shift of the absorption and luminescence bands is revealed when passing from the theoretical models with the para phenylene configuration to the meta one for anthrazoline-containing photoactive moieties (Figs. 2 and 3). For instance, the blueshifts of 26 nm from 410 nm for M1p to 384 nm for M1m (Table 2 and Figure S1). This increase in energy difference of the antibonding LUMO and bonding HOMO-1 orbitals for compounds with *meta*-phenylene configuration in the anthrazoline core can be explained by the loss of conjugation in theoretical models compared to the para-analogues, which leads to lower energies for meta configuration (Table S1). In other words, the double bonding in anthrazoline core with meta-additional phenylene moieties is higher than in the case of para-analogues. For instance, bathochromic effect in absorption spectra for two pairs of Br-substituted meta-isomers (M1m and M6m or M4m and M5m) can be interpreted as a luck of coupling in anthrazoline fragment (Table S1). As a result, Br with has a noticeable $+$ *M*-effect can supply additional electron density to anthrazoline with the expense of slight decrease of bromine electron density.

3.2. Optical properties of experimental models

3.2.1. Low-molecular-mass synthetic models

The absorption and PL spectra of low-molecular-mass synthetic models with para (L1p–L5p) and meta phenylene configuration (L1m–L5m) were recorded in N-methylpyrrolidone (NMP) at concentrations 0.007–0.020 mg/mL (see Section 2.5 and Fig. 3 for details).

3.2.1.1. Absorption. A hypsochromic shift caused by configuration change from para-to *meta*-phenylene configurations for anthrazoline-containing photoactive moieties (Fig. 2a, b, 2c, and 2d) of the absorption and PL bands is revealed according to theoretical models at B3LYP/cc-pVDZ level of theory (Section 3.1). The range of that hypsochromic shift of absorption bands is 37–74 nm, which corresponds to an increase in energy difference between π*-antibonding and π-bonding orbitals in the range of 0.26–0.48 eV. For instance, the largest increase is observed for L3p–L3m pair from 2.62 to 3.10 eV and the smallest increase is for L2p–L2m pair from 2.84 to 3.11 eV (Table 2).

Introduction of two carboxyl (COOH) groups as substituents in the anthrazoline core of L3p-L5p and L3m-L5m (Table 2) leads to a bathochromic shift for both para- and *meta*-phenylene configurations. The maximum shift of 35 nm is observed for transition from L2p to L4p (Table 2). For meta-attachment, the maximum shift, calculated from the difference in absorption band maxima, is only 9 nm for transition from L2m to L5m. The observed effect is related to the nature of –COOH groups with visible negative mesomeric -M effect [33] (Section 3.1). This effect could be weaker in meta-than in para-compounds, which also indicates an initially greater delocalization of the electron density in L1p and L2p in comparison to L1m and L2m, and thus a greater conjugation.

Hypsochromic shift (2 nm, in comparison with L3p) of absorption band maximum is observed when the methyl substituent is introduced into the anthrazoline core, for example, for carboxyl-containing L4p. If carboxyl groups are absent this effect could be greater and equal up to 7 nm for transition from L1p to L2p (Table 2). The effect could be interpreted in terms of $+I_\sigma$ donor properties of methyl group. For anthrazolines with meta phenylene substituents, the methyl group leads to a slight bathochromic shift of 7–8 nm for L3m and L4m and L1m and L2m, respectively. Although even in this case the methyl group possesses $+$ I_σ with Löwdin charge of $+0.05/+0.04$ (Table S3). This opposite effect in the case of *para*-phenylene substituents can be explained by the absence of conjugation at the anthrazoline nucleus in the ground state for L1m–L5m as opposed to para-isomers, as confirmed by theoretical calculations (Figs. 1 and 2; Section 3.1).

Introduction of Br atom in L5p with both –*I* and $+$*M* effects (Section 3.1) lead to a hypsochromic effect at 13 nm compared to L4p (Table 2). However, a bathochromic effect was observed for theoretical models M4p and M5p (Section 3.1). On the other hand, introduction of Br in L5m compared to L4m slightly (by 1 nm) changes position of the absorption band maximum in solution to 408 (Table 2). However, it noticeably shifts its edge to the longwave region (curves 4 and 5, Fig. 3c) in comparison of the 20 nm bathochromic effect for corresponding theoretical models.

3.2.1.2. Photoluminescence. Photoluminescence spectra of synthetic models for anthrazolines with *para*-phenylene substituents demonstrate the same patterns which exist in absorption spectra as well. Introduction of carboxyl groups into anthrazoline core leads to a long-wave shift of the maximum intensity in the emission band up to 85 nm (Fig. 3b and Table 2). PL spectra demonstrate 5 nm hypsochromic shift in the emission band of L1p and L2p or L3p and L4p (Fig. 3 b and Table 2) caused by methylation of the anthrazoline fragment. Introduction of Br leads to a blue shift at 74 nm which is opposite to the action of COOH-substituents (cp. L5p, Lp3 and Lp1 in NMP, Table 2). In addition, the action of the Br-substituent for the synthetic models is opposite to that for the theoretical analogues, where a batochromic shift is observed.

The transition from L1p–L5p para-compounds to their L1m–L5m meta-analogues leads to a noticeable hypsochromic effect in the emission spectra of their solutions accompanied by a shift in the intensity maxima by 80–150 nm (Fig. 3b and d, Table 2). The introduction of CH_3- and COOH-substituents in meta-conformers leads to different behavior in the emission band as compared to the para-analogues. The introduction of a CH3 group into m-compounds (see L1m vs. L2m, Fig. 3d) results in a bathochromic shift of 16 nm compared to p-compounds, which exhibit a hypsochromic shift of 5 nm (see L1p vs. L2p, Fig. 3b–Table 2). The introduction of a COOH substituent results in a bathochromic shift for both m- and p-compounds. However, the magnitude of this shift is less pronounced for L1m and L3m, exhibiting a red shift of only 22 nm (Fig. 3d), and is more pronounced for p-

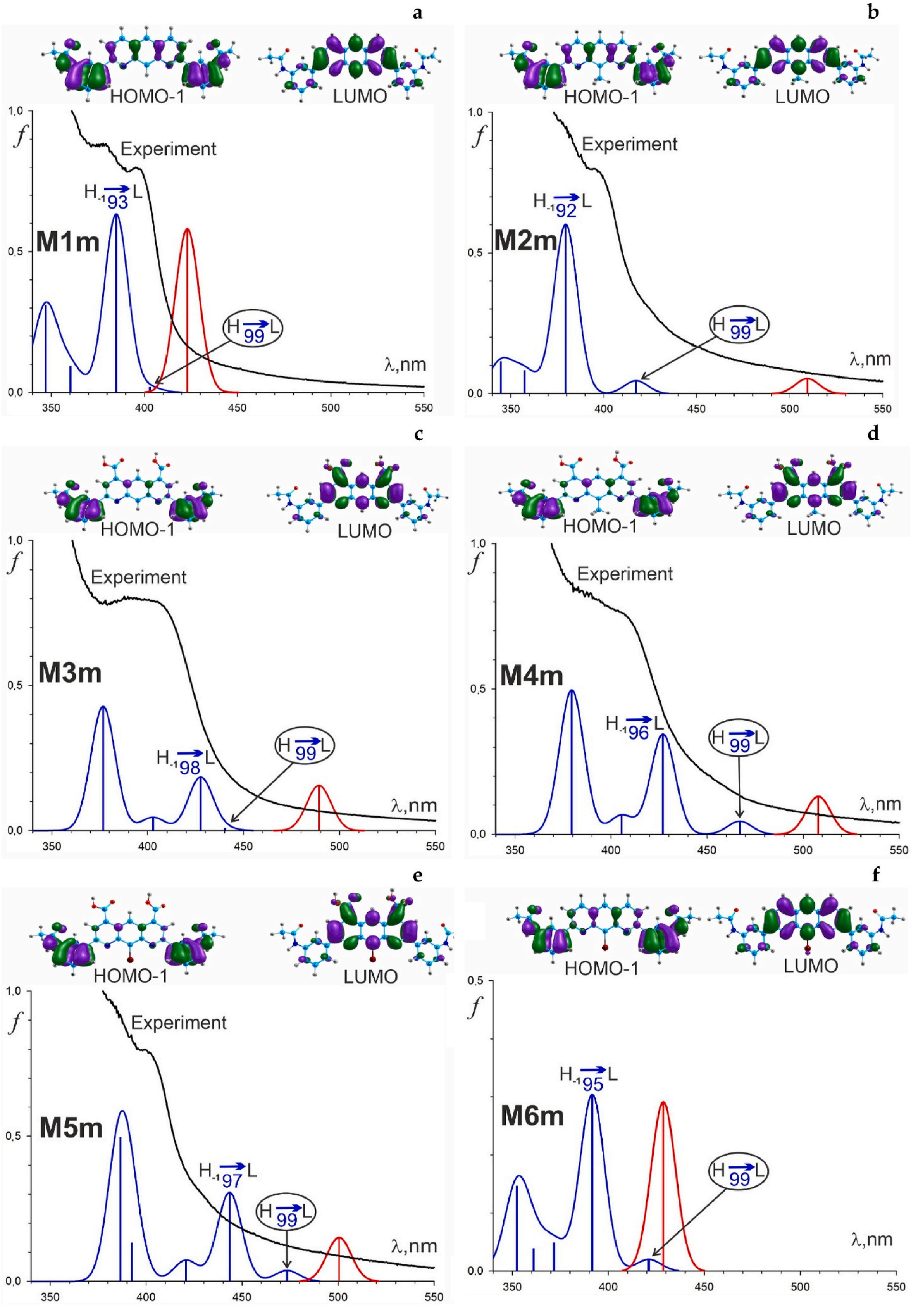

Fig. 2. The theoretical absorption (blue) and emission (red) spectra of M1m–M6m molecules and experimental (black) absorption spectra of P1m–P5m polymers in NMP solution (a–f, respectively). H_{-1} stands for HOMO-1, H is for HOMO, and L is for LUMO orbitals with contribution (%) in different transitions. Oscillator strength, *f*, is in arb. un. Theoretical spectral profiles were simulated using Gaussian functions with a FWHM of 15 nm.

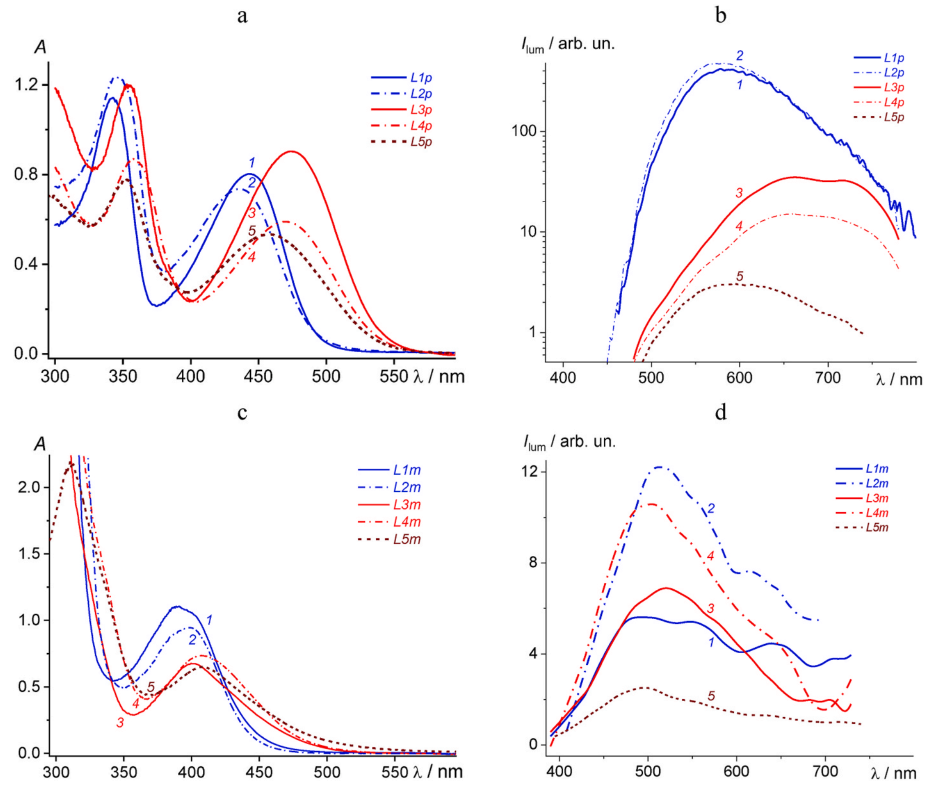

Fig. 3. Absorption (a, c) and photoluminescence (b, d) spectra of for L1p–L5p (a, b) and L1m–L5m (c, d) in NMP at concentrations in the range 0.007–0.02 mg/mL. The excitation wavelengths are 380 nm. The colors indicate moieties before (blue) and after (red) substitution of two carboxylic groups. Spectral lines for Br-substituted moieties indicated in wine.

compounds, exhibiting a red shift of 84 nm (Fig. 3b). Introduction of Br into L4m leads to visible hypsochromic effect of 9 nm in L5m, which is comparable to such an effect in the theoretical M{4,5}m (curves 5 in Fig. 3b and d). The para-configurations demonstrate either significant hypsochromic effect for synthetic models or a bathochromic effect for the theoretical ones. Observed changes in absorption and luminescence spectra caused by introduction of Br suggest dimer formation in solution of L1p–L5p in contrast to their meta-analogues.

3.2.2. *Copolyamides in solution and bulk*

Fig. 4 demonstrates the absorption and luminescence spectra of copolymer solutions P1p|m – P5p|m (analogues of L1p|m – L5p|m and M1p|m – M5p|m), which are coPA of 1,9-anthrazoline (pyrido [3,2-g] quinoline) core attachment through either 4,4′ (para) or 3,3’ (meta) positions of two [(*substituted* carbonyl)amino]phenyl fragments in the polymeric backbone (Section “Synthesized copolyamides” in Electronic Support Materials – ESM).

Fig. 4b shows the absorption and luminescence spectra of poly-{1-[2-methoxy-4-*substituted* phenyl] 4-{2-methoxy-4-[(meta-{8-[meta-([*substituted* carbonyl]amino)-phenyl]pyrido [3,2-g]quinolin-2-yl} phenyl) carbamoyl]phenyl} benzene- 1,4-dicarboxylate} – *co* – {1-[2-methoxy-4-*substituted* phenyl] 4-{2-methoxy-4-[(4-{4-[(*substituted* carbonyl)amino]phenoxy}phenyl) carbamoyl]phenyl} benzene-1,4-dicarboxylate}, or the copolyamide P1m in meta phenylene configuration without auxochromic groups at the anthrazoline (pyrido [3,2-g] quinoline) cores (see Section “Synthesized copolyamides” in ESM). The comparison of the spectra demonstrates their symmetry relative to the 0–0 transition at 415 nm (curves *1*’ and *1*, see arrows). This fact can be attributed to the absorption caused by the anthrazoline fragment. The absorption band of P1m solution contains two distinctive maxima at 395 and 378 nm, which could be attributed to vibronic states. The emission band of P1m solution has three maxima at 427, 447, and 472 nm, corresponding to vibronic states as well.

Let’s compare the optical properties of P1m copolymer with visible spectra of the remaining P2m–P5m copolyamides in NMP (see Section “Synthesized copolyamides” in ESM). The introduction of methyl group in the anthrazoline core, P2m, at position 10 (10-methylpyrido [3.2-g] quinoline) yields a redshift from 412 to 425 nm as compared to the P1m on an absorbance band edge (see the dash level at A = 0.3, Fig. 4b). In this case, no bathochromic shift of the long wavelength maxima at 395 nm in an absorbance band is observed (curves *1*′ and *2*′, Fig. 4b). The luminescence band for P2m solution experiences a bathochromic shift 16 nm from 427 to 443 nm for short-wavelength shoulders relative to P1m. The same absorbance bathochromic effect from 433 to 437 nm is observed for the pair of P3m/P4m without and with methyl groups and two carboxyl groups in anthrazoline units, namely 4,6-dicarboxylpyrido [3,2-g]quinoline and 10-methyl-4,6-dicarboxylpyrido [3,2-g]quinoline.

Introduction of two carboxyl groups to anthrazoline unit leads to a significant decrease (4.8 times) of luminescence intensity of P3m solution in comparison with P1m (curves *3* and *1*, Fig. 4b). A significant bathochromic shift of the long-wavelength edge of the absorption band is observed, namely from 412 to 433 nm, where the edge value is taken at the optical density equal to 0.3 (curves *1*′ and *3*’ at the dash line level in Fig. 4b). The P3m luminescence band is structureless and has a redshift maximum at 494 nm as compared with the 447-nm maximum in the vibronic structure of P1m band (Table 2). The introduction of the methyl radical along with two carboxyl groups in P4m as compared with P2m conserves the luminescence efficiency as opposed to the situation for P3m and P1m solutions (see above). At that, the main maximum in the luminescence band shifts to the long-wavelength region from 467 to 503 nm (Table 2).

Introduction of Br instead of the methyl group in the P5m anthrazoline core (10-bromo-4,6-dicarboxylpyrido [3,2-g]quinoline) does not conserve the luminescence efficiency in contrast with P4m case (Fig. 4b). In this case, the luminescence intensity drops by a factor of 3.6 as compared with P1m. The absorbance band of P5m solution

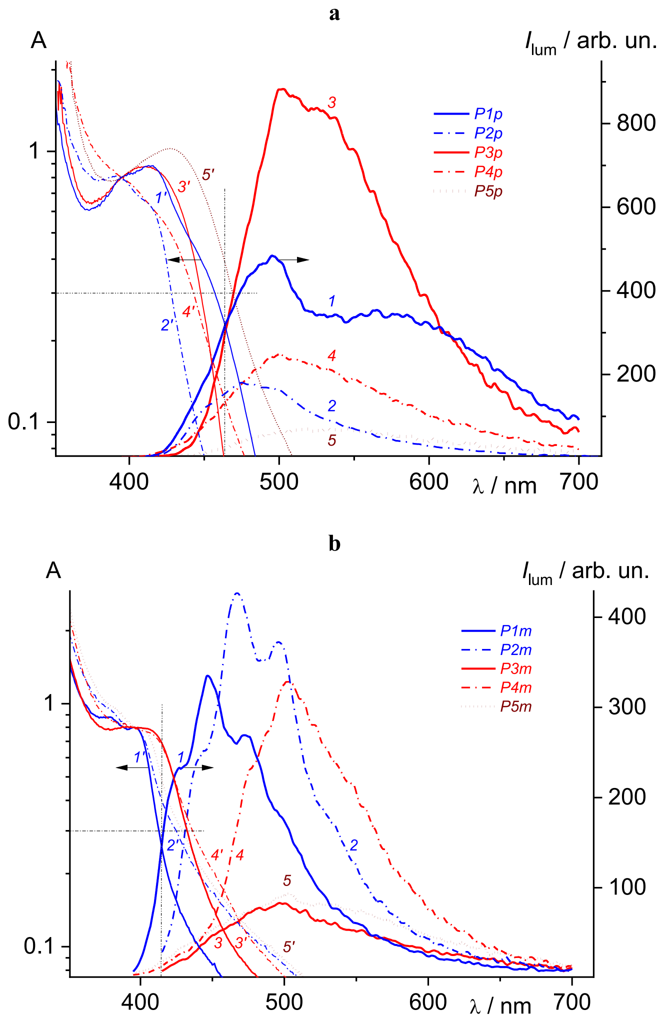

Fig. 4. Absorption (excitation wavelength 380 nm) (*1′*–*5′*) and luminescence (*1*–*5*) spectra of copolyamides P1p–P5p (a) and P1m–P5m (b) in NMP. $c_{\mathrm{pol}} =$ 0.62 g/L. Blue and red colors correspond to the moieties either with or without two carboxylic groups. Wine color correspond to Br-substituted moiety. The horizontal dashed line corresponds to absorbance A = 0.3, whereas the vertical dashed line at 415 nm indicates curves *1* and *1′* symmetry.

experiences a bathochromic shift as compared with P1m from 412 to 430 nm (cp. Curves *1′* and *5′* at the dash line level in Fig. 4b). In this case, there is also the hypsochromic shift to 430 nm as compared with P3m (433 nm) oppositely to the red shift of P4m (437 nm) (curve *4*' at the dash line level, Table 2).

So, the absorption spectra in the region of 370–550 nm turn out to be indicative of the excited electronic states of the anthrazoline core (Figs. 1, 3 and 4). Fig. 4a shows the absorption and luminescence spectra for copolyamides with the *para* phenylene configuration in anthrazoline-containing mer, e. g. for poly-{1-[2-methoxy-4-*substituted* phenyl] 4-{2-methoxy-4-[(para-{8-[para- ([*substituted* carbonyl]amino)-phenyl] pyrido [3,2-g]quinolin-2-yl}phenyl) carbamoyl]phenyl} benzene-1,4-dicarboxylate} – *co* – {1-[2-methoxy-4-*substituted* phenyl] 4-{2-methoxy-4-[(4-{4- [(*substituted* carbonyl)amino]phenoxy} phenyl)carbamoyl]phenyl} benzene-1,4-dicarboxylate}, or copolyamide P1p, which has no substituents in the anthrazoline core (see Section “Synthesized copolyamides” in ESM).

The transition from meta-to para-configuration of the phenylene fragments relative to anthrazoline core in copolyamides was found to exhibit a bathochromic shift in both absorption and emission bands (Fig. 4a and b). For example, for P1m→P1p pair, the absorption band maximum shifts from 395 to 414 nm (P1p|m–P5p|m in NMP rows, Tables 2 and 3), as well as for emission band from 447 to 495 nm. This PNm→PNp shift for coPA is also comparable to that observed for theoretical MNm→MNp models with similar shifts for M1m and M1p pair in absorption band from 379 to 410 nm and in the emission band from 426 to 471 nm (M1p|m–M6p|m rows, Table 2). In coPA one might attribute the observed bathochromic effect to greater delocalization of electron density in anthrazoline-containing SRU in *para*-phenylene configuration compared to meta-one (Figs. 2 and 3) (see theoretical models).

However, it turned out that for low-molecular-mass synthetic models this shift is much larger. For example, in absorption band for L1m and L1p the observed shifts are from 391 to 443 nm, and in emission band from 498 to 578 nm. Thus, comparing the solutions of PNp copolymers with low-molecular-mass synthetic analogues of LNp, the observed magnitudes of maxima in absorption and emission bands are shifted to the short-wave region. For example, in the absorption spectrum for L1p the maximum is observed at 443 nm and for P1p the maximum is observed at 414 nm. In emission spectrum, the maximum for L1p is located at 578 nm and for P1p is located at 495 nm (Table 2). The maxima in absorption bands for the theoretical models (MNm) and coPA (PNm) in meta-configuration of phenylene fragments in anthrazoline-containing mers coincide to each other (Table 2). To explain these effects, the maxima in emission and absorption bands of low-molecular-mass synthetic compounds with para-configuration (LNp) can be matched to the dimers formed by the corresponding small molecules.

For copolymers, the dimer luminescence peaks have visible intensities except P1p solutions (row P1p-P5p in NMP, Table 2, curve 1, Fig. 4a). It could be caused by probable steric hindrances in intra-macromolecular interactions of the anthrazolinic fragments. Copolyamides are rigid-chain polymers due to the presence of extended aromatic fragments in the main polymer chain (Fig. S6). Thermodynamic flexibility leads to depletion of conformations in which interactions of distant contacts along the chain occur, which could contribute to the formation of dimers.

The absorption and luminescence spectra show that the introduction of two carboxyl substituents to the anthrazoline core (4,6-dicarboxylpyrido [3, 2-g]quinoline) leads to a bathochromic shift of the spectral bands of P3p (4,6-dicarboxylpyrido [3,2-g]quinoline) and P4p (10-methyl-4,6-dicarboxylpyrido [3,2-g]quinoline) relative to P2p (Fig. 4a) which was attributed (see above) to negative mesomeric effect of carboxyl groups. In contrast to PNms, for P1p solution the absorption band lies in red-wave region relative to the P3p and P4p. This bathochromic shift indicates dimer formation in the solution. For P2p–P4p, dimer formation is ineffective, which may be due to steric hindrances and possible electronic changes in the anthrazoline core.

The introduction of a donor methyl group at position 10 of anthrazoline core (10-methylpyrido [3.2-g]quinoline) in copolymer P2p instead of electron-withdrawing groups leads to a little hypsochromic effect for short-wavelength maxima in the absorbance spectra as compared with P1p from 399 to 391 nm. So, for para-configuration the CH_3-substituent with +*I* effect [33] increases the electron density localization at anthrazoline core and thereby the bond order and multiple bond localization for para-configuration in opposite to meta-configuration, for which the group promotes delocalization of anthrazoline core electron density. Thus, benzene rings attached to positions 2 and 8 of the anthrazoline core, depending on either para- or meta-configuration in a polymer backbone (2,8-bis-{*para*-|*meta*-[(*substituted* carbonyl)amino]phenyl}pyrido [3,2-g]quinoline) exhibit a negative inductive effect being essentially an electron acceptor [33].

Introduction of three substituents like two carboxy groups and bromine into anthrazoline core results in bathochromic shift observed in absorption spectrum of P5p copolymer (10-bromo-4,6-dicarboxylpyrido [3,2-g]quinoline) in respect to P3p (4,6-dicarboxylpyrido [3,2-g] quinoline) with shift of the maximum from 411 to 428 nm. This can be attributed to further delocalization of the electron density in P3p, P4p and P5p series since bromine has –*I* and +*M* effects [33]. Quantum-chemical calculations show a positive Löwden atomic charge localized at Br (Table S2). As noted above, the meta-configuration of phenylene groups enhances the effect of electron delocalization at anthrazoline core due to the attachment of an additional auxochrome, which has donor properties. This manifests itself in the bathochromic effect in the absorption and emission spectra.

Fig. 5 demonstrates the luminescence spectra of P1p–P5p and P1m–P5m films which indicate a probability of the dimer formation caused by strengthening of a polymer–polymer interaction instead of polymer–solvent bonds. In comparison with NMP solutions, this phenomenon manifests itself as increased contribution of the long-wavelength band around 600 nm for P1p–P5p (Fig. 5a and a). It is particularly evident for P1p film, for which luminescence spectrum remains only the 570–700 nm band with emission maximum at 638 nm. The effect could be related to the dimer formation caused by van der Waals interaction. The formation of dimers rather than exciplexes is proved by the fact that in P1p solution the shoulder at 457 nm appears in the absorption spectra, and dimer luminescence has the add-on maximum intensity in the emission band at 576 nm (curve 1, Fig. 4a) as well. For P2p film, the band contribution at 581 nm is enhanced compared to short-wavelength region of 450–520 nm. In addition, in P2p solution, the luminescence band has a maximum at 476 nm and a long-wave shoulder at 550 nm. However, the contribution of this shoulder in solution is much lower than in the film, because in solution the conformation of the polymer coil formed by inflexible macromolecules of anthrazoline-containing coPAs does not allow dimer formation to occur efficiently, and there are no intermacromolecular interactions inherent to the polymer film. In addition, as it was shown for P2p and P4p films (Fig. S4), a decrease in concentration of anthrazoline fragments affects the redistribution of low- and high-energy contributions in a luminescence band. As far as P5p concerned, its luminescent band undergoes a bathochromic shift during transition from solution to film, with a maximum shift from 545 to 619 nm (Table 2).

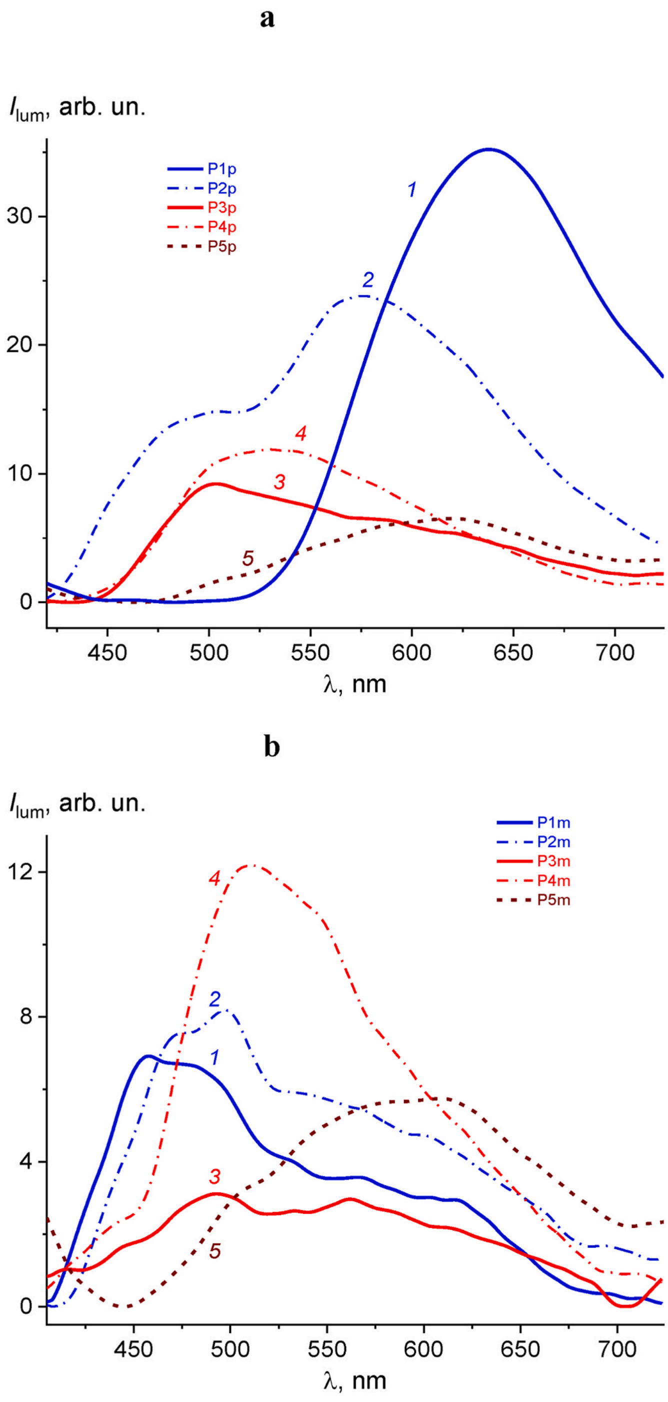

Fig. 5. Luminescence spectra of the films of copolymers P1p–P5p (a) and P1m–P5m (b) with excitation wavelength 380 nm.

Theoretical M1m, M2m, and M3m absorption and luminescence spectra of meta-configurations do not demonstrate good agreement with correspondent L1m, L2m, and L3m spectra in solution (Table 2, Fig. S5). For instance, L1m and L2m absorption and luminescence spectra are shifted to the long-wavelength region compared to the maxima of M1m and M2m. For L3m solution, a shoulder at 430 nm is observed with corresponding M3m theoretical absorption maximum at 428 nm, and the maxima in emission band for L1m–L3m solutions are shifted to the long-wavelength spectral region compared to M1m–M3m.

Both luminescence theoretical M4m and M5m spectra coincide well with experimental ones of low-molecular-mass compounds L4m and L5m (Figs. S5 and d). The theoretical and experimental absorption spectra of these two compounds are close to each other if we consider the shoulders in the experimental ones (Table 2). It allows one to speculate about applicability of TD/SMD/B3LYP/cc-pVDZ DFT to calculate atomic and electronic structure and optical spectra of anthrazoline-containing moieties. Taking into account the above findings, one can speculate about a possibility of formation of luminescent dimers in NMP solutions of unconjugated meta-configurations of L1m and L2m and excimers in L3m NMP solution due to van-der-Waals interactions in unconjugated meta-configuration of low-molecular-mass compounds without large substituents in their cores with the formation of “sandwich” structures. The introduction of two sufficiently bulky carboxyl groups in L3m anthrazoline fragment leads to the formation of excimers only, as it is due to conjugated configurations in the excited state (Fig. 2). Further intensification of steric hindrances for the interaction of anthrazolinic fragments due to either auxochromic $-CH_3$ (L4m) or -Br (L5m) groups eliminate dimer or excimer formation in the organic solvent.

It should be noted that theoretical TD/SMD/B3LYP/cc-pVDZ approach correctly predicts the energy positions of maxima and shoulders in both absorption and luminescent spectra of meta configuration of P1m – P5m copolymers in NMP solutions (Fig. 4b–Table 2) with distinctive bathochromic shifts for anthrazoline copolymers in NMP solution in comparison with M1m–M5m ones. It means that in solution the anthrazoline-containing SRU in meta-configurations behave quite individually because of weak interactions between distant similar monomers along the polymer chain. The strengthening of intermacromolecular interactions between chromophore groups can be observed only in films using luminescence spectra (Fig. 5b–Table 2). In P1m–P5m luminescence spectra, a decrease of the contribution of 420–520 nm band as compared to the 550–670 nm one is observed when transferring from solution to film (Figs. 4b and 5b). This effect could be interpreted as an increase of the probability of either dimer or excimer formation between anthrazolinic SRU in copolymers and depletion of direct luminophore emission channel.

The emission maxima of para-configuration theoretical models (M1p – M5p) show a poor correlation with the experimental luminescence spectra of low-molecular-mass compounds (L1p – L5p) in NMP. The difference in peak positions can be as high as 33 nm in the long-wavelength spectral region, as detailed in Table 2. This is detected because of formation of dimeric associates caused by π–π-interactions of aromatic fragments of L1p – L5p in NMP. This effect could manifest itself as a shift of spectral maxima to long-wavelength region in comparison with free-standing molecules [34]. The maxima in absorption spectra of the two P1p and P2p coPAs in solution are consistent with theoretical M1p and M2p in the absorption band with distinctive long-wavelength shoulder with broad emission band with several long-wavelength maxima and shoulders at 576 (P1p) and 550 nm (P2p) (Table 2). This fact points to the formation of dimers in polymer solutions due to the possible interactions of the co-monomeric units.

The luminescence spectra of P3p, P4p, and P5p in NMP solutions correspond well to theoretical M3p, M4p, and M5p luminescence spectra (Fig. 4). Normalized absorption spectra of coPA display long wavelength tails at $A = 0.3$, which correspond well to theoretical maxima (Table 2). It could be interpreted as a steric hindrance caused by the multiple and bulky substituents in anthrazolinic nucleus which interferes with the efficient formation of dimers.

At TD/SMD/B3LYP/cc-pVDZ DFT levels of theory absorption spectral maxima for theoretical models are formed by HOMO-1−LUMO transitions. The LUMO electron density is mainly localized at anthrazoline fragments and carboxyl groups. However, the formation of HOMO-1 also involves electronic states localized on different groups, such as anthrazoline-core states for predominantly meta-configuration phenylene moieties with some density at para-configurations as well. For para-configuration of phenylene, electronic transitions involve electronic states localized just at one anthrazoline core and require less energy than transitions between different moieties, such as benzene rings and anthrazoline core in the case of meta-configuration of phenylene (Figs. 2 and 3). Therefore, the absorption and luminescence spectra of the compounds with para-substituted phenylenes demonstrate visible red shifts relative to meta-compounds.

The energy positions of maxima and shoulders in *meta*-coPA films emission bands coincide well with corresponding theoretical values (Table 2) whereas para-compounds do not reveal such spectral features. This could be interpreted as a spectral manifestation *meta*-anthrazoline monomers and *para*-anthrazoline dimers, respectively. Indeed, the luminescence spectra of coPA films reflect possible interactions of chromophore groups leading to π-stacking and dimers and bulk excimers formation (Fig. S6) Various supramolecular structures can be formed either in solution or copolymer films. Furthermore, the polymer−polymer interactions between distant groups along the chain dominate in the solutions, whereas in bulk, the polymer−polymer interactions are supported essentially by intermacromolecular interactions. This becomes quite clear when comparing the luminescence spectra of the solutions and films (Figs. 4 and 5).

4. Conclusions

Using TD/SMD/B3LYP/cc-pVDZ electronic structure calculations it was shown that absorption spectra of the para-versus meta-theoretical models of 2,8-bis-[*para*-|*meta*-(methcarbonylamino)phenyl]pyrido [3,2-g]quinoline demonstrate visible red shifts which coincide well with corresponding experimental spectra. It was found that absorption and luminescence spectra of para- M2p, L2p, and P2p demonstrate minor hypochromic shifts of long-wavelength absorption and short-wavelength emission maxima in respect to M1p, L1p, and P1p. In respect to the compounds without substituents, the absorption spectra of M3p–M4p, L3p–L4p, and P3p–P4p demonstrate ~30 nm experimental bathochromic shifts in comparison with ~60 nm of theoretical ones. Bothe theoretical and experimental luminescence spectra demonstrate bathochromic shifts up to 50 nm in solutions and copolymer solutions. Similar behavior of the spectra was also observed for compounds in the meta configuration. It was shown that both emission and absorption spectra of low-molecular-mass synthetic and theoretical models demonstrate similar effect of substituents in the anthrazoline cores in a copolyamide solutions. It was established that two phenyl groups either in meta- or para-positions to polymeric chain exhibit negative inductive effect to the nature of electron delocalization. The presence of additional shoulders in emission spectra of all para-low-molecular-mass synthetic models and *para*-coPA in solution suggests a possibility of dimer formation. Some disagreements between theory and experiment for low-molecular-mass compounds could be caused by formation of van der Waals dimers in solutions. It was shown that the dimers have a significant bathochromic spectral shift compared to the monomers. The discrepancy between spectroscopic theoretical and experimental data for polymers was interpreted as manifestation of polymer effects caused by intra- and intermolecular interactions. It was shown that theoretical spectra coincide well with experimental spectroscopic data which directly indicates that at TD/SMD/B3LYP/cc-pVDZ level of theory can be used to study atomic and electronic structure of non-conjugated anthrazoline coPA compounds allowing one to establish trends in shifting of absorption and luminescence bands for the conjugated of phenylene substituents with auxochromic groups in polymer chains. The TD/SMD/B3LYP/cc-pVDZ approach provides an accurate deconvolution of both experimental absorption and luminescence spectra highlighting $S_0 \rightarrow S_1$ electronic transitions against spectral background which is formed by Förster resonance energy transfer, complex vibrational structure, intra- and intermolecular complexes with charge transfer.

Supplementary Materials: Table S1: Energies of absorption $S_0 \rightarrow S_1$ transitions for theoretical models M1p–M5p and M1m–M5m; Table S2: Theoretical Löwdin atomic charges (e) localized at para-configurations of phenylene (M1p–M6p) in anthrazoline fragments; Table S3: Löwdin charges (e−) localized at structural of M1m–M6m models with para-configurations of phenylene in anthrazoline fragments; Table S4: Values of the centers of gravity of the x_c peaks obtained by approximation with the *Asym2Sig* function in the absorption spectra of model compounds L1p–L4p. Comparison with quantum-chemical calculation; Table S5: Hypsochromic (bathochromic) shifts during the transition from meta to para configuration of phenylene groups in low molecular weight L1-5p|m models in solution; Fig. S1: Chemical structure of the low-molecular-mass synthetic models with the para-(L1p—L5p) and *meta*-phenylene configurations (L1m—L5m) in anthrazoline fragments; Fig. S2: Calculation scheme; Fig. S3: Deconvolution of absorption spectra of low molecular mass synthetic L1p–L4p models. Fig. S4: Luminescence spectra of copolyamide films with *para*-attachment of phenylene moieties and methylation of anthrazoline fragment (curves *1*′, *2*′, and *3*′), and addition carboxylation (curves *1*, *2*, and *3*) at varying the content of anthrazoline fragment: 5 (*1* and *1*′), 10 (*2* and 2′) and 90 % (*3* and *3*′); Fig. S5: Comparison of the theoretical and experimental spectra maxima of the compounds with the para (a,b) and meta phenylene (c,d) configurations in anthrazoline fragments; Fig. S6: Possible “hairpin” conformation for the A-B fragment in the P2m copolyamide corresponding to the low molecular weight luminophore L2m. Visualization and optimization of the molecule in Samson program.

Funding

Felix N. Tomilin and Sergei G. Ovchinikov within the state assignment of Kirensky Institute of Physics, Irina A. Shchugoreva, Polina V. Artyushenko, and Anastasia V. Rogova appreciates the Ministry of Science and Higher Education of the Russian Federation for funding the study, project no. FWES-2022-0005. Molecular design of anthrazoline derivatives was supported by the National Research Foundation of the Republic of Korea, grant NRF 2021R1A2C1010455.

CRediT authorship contribution statement

Irina A. Shchugoreva: Writing – review & editing, Writing – original draft, Visualization, Validation, Software, Investigation, Formal analysis, Data curation, Conceptualization. **Ruslan Y. Smyslov:** Writing – review & editing, Writing – original draft, Visualization, Validation, Supervision, Software, Project administration, Investigation, Formal analysis, Data curation, Conceptualization. **Irina A. Nasirova:** Writing – review & editing, Writing – original draft, Methodology, Investigation. **Mikhail Y. Goikhman:** Project administration, Methodology, Conceptualization. **Alexander V. Yakimansky:** Writing – review & editing, Resources, Funding acquisition. **Sergei G. Ovchinikov:** Writing – review & editing, Resources. **Polina V. Artyushenko:** Software. **Anastasia V. Rogova:** Software. **Felix N. Tomilin:** Writing – review & editing, Writing – original draft, Visualization, Validation, Supervision, Software, Resources, Project administration, Methodology, Investigation, Funding acquisition, Formal analysis, Data curation, Conceptualization. **Pavel V. Avramov:** Writing – review & editing.

Declaration of competing interest

The authors declare that they have no known competing financial interests or personal relationships that could have appeared to influence the work reported in this paper.

Data availability

Data will be made available on request.

Acknowledgments

The authors thank the Joint Supercomputer Center of the Russian Academy of Sciences (JCSS of RAS) for providing computer simulations.

Appendix A. Supplementary data

Supplementary data to this article can be found online at https://doi.org/10.1016/j.optmat.2024.116135.

References

[1] P.P. Manousiadis, K. Yoshida, G.A. Turnbull, I.D.W. Samuel, Organic semiconductors for visible light communications, Phil. Trans. R. Soc. A. 378 (2020) 20190186, https://doi.org/10.1098/rsta.2019.0186.

[2] H. Liu, D. Liu, J. Yang, H. Gao, Y. Wu, Flexible electronics based on organic semiconductors: from patterned assembly to integrated applications, Small 19 (2023) 2206938, https://doi.org/10.1002/smll.202206938.

[3] Organic Field-Effect Transistors, Z. Bao, J.J. Locklin (Eds.), Optical Science and Engineering, CRC Press, Boca Raton, 2007. ISBN 978-0-8493-8080-8.

[4] H. Kim, N. Schulte, G. Zhou, K. Müllen, F. Laquai, A high gain and high charge carrier mobility indenofluorene-phenanthrene copolymer for light amplification and organic lasing, Adv. Mater. 23 (2011) 894–897, https://doi.org/10.1002/adma.201003797.

[5] C. Wang, H. Dong, W. Hu, Y. Liu, D. Zhu, Semiconducting π-conjugated systems in field-effect transistors: a material odyssey of organic electronics, Chem. Rev. 112 (2012) 2208–2267, https://doi.org/10.1021/cr100380z.

[6] C. Liu, L. Shao, S. Chen, Z. Hu, H. Cai, F. Huang, Recent progress in π-conjugated polymers for organic photovoltaics: solar cells and photodetectors, Prog. Polym. Sci. 143 (2023) 101711, https://doi.org/10.1016/j.progpolymsci.2023.101711.

[7] S.B. Mdluli, M.E. Ramoroka, S.T. Yussuf, K.D. Modibane, V.S. John-Denk, E. I. Iwuoha, π-Conjugated polymers and their application in organic and hybrid organic-silicon solar cells, Polymers 14 (2022) 716, https://doi.org/10.3390/polym14040716.

[8] C.-H. Chang, K.-C. Tien, C.-C. Chen, M.-S. Lin, H.-C. Cheng, S.-H. Liu, C.-C. Wu, J.-Y. Hung, Y.-C. Chiu, Y. Chi, Efficient phosphorescent white OLEDs with high color rendering capability, Org. Electron. 11 (2010) 412–418, https://doi.org/10.1016/j.orgel.2009.11.020.

[9] T.W. Kwon, A.P. Kulkarni, S.A. Jenekhe, Synthesis of new light-emitting donor–acceptor materials: isomers of phenothiazine–quinoline molecules, Synth. Met. 158 (2008) 292–298, https://doi.org/10.1016/j.synthmet.2008.01.017.

[10] B. Huang, J. Li, Z. Jiang, J. Qin, G. Yu, Y. Liu, New series of light-emitting polyquinolines containing 9,9‘-spirobifluorene units, Macromolecules 38 (2005) 6915–6922, https://doi.org/10.1021/ma050741q.

[11] Q. Zhang, P. Jiang, K. Wang, G. Song, H. Zhu, The synthesis, crystal structures and photophysical properties of a series of novel 4,6-diphenyl-1,9-anthrazolines, Dyes Pigments 91 (2011) 89–97, https://doi.org/10.1016/j.dyepig.2011.02.011.

[12] C.J. Tonzola, M.M. Alam, W. Kaminsky, S.A. Jenekhe, New N-type organic semiconductors: synthesis, single crystal structures, cyclic voltammetry, photophysics, electron transport, and electroluminescence of a series of diphenylanthrazolines, J. Am. Chem. Soc. 125 (2003) 13548–13558, https://doi.org/10.1021/ja036314e.

[13] M.Ya Goikhman, I.A. Valieva, I.V. Podeshvo, I.V. Gofman, R.Yu Smyslov, L. S. Litvinova, A.V. Yakimansky, Synthesis and photoluminescence properties of Co-polyamides with anthrazoline-containing units in the main chain, Luminescence 33 (2018) 559–566, https://doi.org/10.1002/bio.3446.

[14] G.C. Dos Santos, V.F. Moreno, B.H.S.T. Da Silva, L.C. Da Silva-Filho, Heterocyclic anthrazoline derivatives: a critical review, New J. Chem. 43 (2019) 18415–18432, https://doi.org/10.1039/c9nj04995a.

[15] A.J. Heeger, Light emission from semiconducting polymers: light-emitting diodes, light-emitting electrochemical cells, Lasers and white light for the future, Solid State Commun. 107 (1998) 673–679, https://doi.org/10.1016/S0038-1098(98)00215-4.

[16] V. Bhat, C.P. Callaway, C. Risko, Computational approaches for organic semiconductors: from chemical and physical understanding to predicting new materials, Chem. Rev. 123 (2023) 7498–7547, https://doi.org/10.1021/acs.chemrev.2c00704.

[17] H. Bronstein, C.B. Nielsen, B.C. Schroeder, I. McCulloch, The role of chemical design in the performance of organic semiconductors, Nat. Rev. Chem 4 (2020) 66–77, https://doi.org/10.1038/s41570-019-0152-9.

[18] F.A. AL-Temimei, H.A.A. Mraity, DFT/TD-DFT investigation of novel D–π–A configuration dyes for improving solar cell efficiency, Struct. Chem. 33 (2022) 859–869, https://doi.org/10.1007/s11224-022-01901-7.

[19] A. Picot, C. Feuvrie, C. Barsu, F. Malvolti, B. Le Guennic, H. Le Bozec, C. Andraud, L. Toupet, O. Maury, Synthesis, structures, optical properties, and TD-DFT studies of donor-π-conjugated dipicolinic acid/ester/amide ligands, Tetrahedron 64 (2008) 399–411, https://doi.org/10.1016/j.tet.2007.10.064.

[20] S. Gümüş, M. Akbay, A computational study on substituted and unsubstituted mono and diazaanthracenes, Polycycl. Aromat. Comp. 33 (2013) 519–532, https://doi.org/10.1080/10406638.2013.816975.

[21] Gleiter, R.J.A. Barltrop, J.D. Coyle, Excited states in organic chemistry, J. Wiley and sons, ltd. 1975, 365 seiten, preis: £ 15, Ber Bunsenges Phys Chem 80 (1976) 466, https://doi.org/10.1002/bbpc.19760800519, 466.

[22] R.Y. Smyslov, F.N. Tomilin, I.A. Shchugoreva, G.I. Nosova, E.V. Zhukova, L. S. Litvinova, A.V. Yakimansky, I. Kolesnikov, I.G. Abramov, S.G. Ovchinnikov, et al., Synthesis and photophysical properties of copolyfluorenes for light-emitting applications: spectroscopic experimental study and theoretical DFT consideration, Polymer 168 (2019) 185–198, https://doi.org/10.1016/j.polymer.2019.02.015.

[23] I.A. Valieva, M.Ya Goikhman, I.V. Podeshvo, N.L. Loretsyan, I.V. Gofman, R. Yu Smyslov, L.S. Litvinova, A.V. Yakimansky, Copolyamides based on anthrazoline-containing diamines: synthesis and properties, Polym. Sci. B 61 (2019) 302–308, https://doi.org/10.1134/S1560090419030163.

[24] M.Y. Goikhman, I.V. Podeshvo, G.M. Mikhailov, Y.G. Baklagina, V.V. Kudryavtsev, S.V. Lukashov, M.F. Lebedeva, N.V. Bobrova, Y.N. Sazanov, G.N. Fedorova, M. V. Mikhailova, I.P. Deineko, A new bifunctional monomer, terephthaloylbis(3-methoxy-4-oxybenzoyl) dichloride, and polyamides prepared from it, Russ. J. Appl. Chem. 70 (1997) 1793–1797. https://scholar.google.com/scholar?hl=en&as_sdt=0%2C5&q=Russ.+J.+Appl.+Chem.+1997%2C+70%2C+1793%E2%80%931797.&btnG=, 2024.

[25] OriginPro, (64-bit), build 10.1.5.132, from OriginLab corporation. https://www.originlab.com/, 2024.

[26] A.D. Becke, Density-functional thermochemistry. III. The role of exact exchange, J. Chem. Phys. 98 (1993) 5648–5652, https://doi.org/10.1063/1.464913.

[27] A.V. Marenich, C.J. Cramer, D.G. Truhlar, Universal solvation model based on solute electron density and on a continuum model of the solvent defined by the bulk dielectric constant and atomic surface tensions, J. Phys. Chem. B 113 (2009) 6378–6396, https://doi.org/10.1021/jp810292n.

[28] F. Neese, Prediction of molecular properties and molecular spectroscopy with density functional theory: from fundamental theory to exchange-coupling, Coord. Chem. Rev. 253 (2009) 526–563, https://doi.org/10.1016/j.ccr.2008.05.014.

[29] M.W. Schmidt, K.K. Baldridge, J.A. Boatz, S.T. Elbert, M.S. Gordon, J.H. Jensen, S. Koseki, N. Matsunaga, K.A. Nguyen, S. Su, et al., General atomic and molecular electronic structure system, J. Comput. Chem. 14 (1993) 1347–1363, https://doi.org/10.1002/jcc.540141112.

[30] P.V. Avramov, A.V. Kuklin, Topological and quantum stability of low-dimensional crystalline lattices with multiple nonequivalent sublattices, New J. Phys. 24 (October 14, 2022) 103015, https://doi.org/10.1088/1367-2630/ac93a9.

[31] Marvin version 23.5.0, ChemAxon. (accessed on the 5th of June, 2024)Available online: https://www.chemaxon.com.

[32] K. Jug, A new definition of atomic charges in molecules, Theor. Chim. Acta 31 (1973) 63–73, https://doi.org/10.1007/BF00527439.

[33] H.G.O. Becker, Einführung in die elektronentheorie organisch-chemischer reaktionen, VEB Deutscher Verlag der Wissenschaften, Berlin, 1974.

[34] C.-C. Teng, C.-C.M. Ma, C.-H. Lu, S.-Y. Yang, S.-H. Lee, M.-C. Hsiao, M.-Y. Yen, K.-C. Chiou, T.-M. Lee, Thermal Conductivity and Structure of Non-covalent Functionalized Graphene/epoxy Composites, vol. 49, 2011, pp. 5107–5116, https://doi.org/10.1016/j.carbon.2011.06.095.